

1 **Phylogenomics and the origins of sharks**

2 Chase Doran Brownstein^{1,2*} and Thomas J. Near^{1,3}

3 ¹Department of Ecology and Evolutionary Biology, Yale University, New Haven CT, USA

4 ²Stamford Museum and Nature Center, Stamford CT, USA

5 ³Yale Peabody Museum, New Haven CT, USA

6 *Corresponding author, chase.brownstein@yale.edu

7 8 **Abstract.**

9 Genomes have the capacity to drastically modify hypotheses about the relationships of species.
10 Despite the growing availability of non-model organism genome sequences, historically
11 contentious portions of Tree of Life remain untested using genomic data. Here, we infer the
12 phylogeny of sharks, skates, rays, and chimaeras using the genomes of 48 species, targeting
13 different genomic marker types. Although phylogenetic relationships of chondrichthyans are
14 relatively consistent across analyses, different molecular markers yield conflicting results about
15 shark monophyly. Exons support the traditional view that sharks are monophyletic, whereas
16 ultraconserved elements and legacy nuclear markers instead suggest that the frilled and cow
17 sharks (*Hexanchiformes*), which retain the ancestral jaw structure of cartilaginous fishes, is the
18 sister lineage of all other sharks and rays. The resolution of sharks as monophyletic or
19 paraphyletic has little effect on inferences of the timescale of shark evolution or the origins of
20 key traits, such as their ancestral ecology and genome size. We tie the diversification of living
21 cartilaginous fishes to the transformation of marine ecosystems during the middle Mesozoic Era,
22 confirming that living shark diversity is the product of rapid ancient diversification.
23 Consequently, our results suggest that despite uncertainty around whether sharks are
24 monophyletic, consensus can still be reached about major evolutionary events in this iconic
25 vertebrate lineage.

26 27 **Significance Statement.**

28 Living sharks, skates, rays, and chimaeras form one of the three principal groups of vertebrates.
29 These iconic animals, which include over 1200 species, are key components of marine
30 ecosystems and have helped us reconstruct the evolution of vertebrate genomes and phenotypes.
31 However, much work on this group has assumed that sharks are a natural group. Here, for the
32 first time, we leverage genome-scale data to test this hypothesis. Surprisingly, we show different
33 genome regions reject or support hypothesis that sharks form a natural group to the exclusion of
34 skates and rays. This throws an unexpected wrench into our understanding of the relationships of
35 some of the oldest living vertebrate clades.

36 37 **Introduction.**

38 Genome-scale data has revolutionized our understanding of the phylogeny of animals (1–
39 5) and their principle clades, especially vertebrates and their closest relatives among chordates
40 (6–11, 11–15). Only recently have the historically contentious (16–21) relationships of the
41 earliest vertebrate divergences been tested using genomic data (22, 23). This region of the
42 vertebrate tree, which includes the successive divergences among jawed and jawless taxa and
43 cartilaginous and bony fishes, is notable for being location of origin for numerous innovations,
44 including the mobile jaw, paired appendages, lungs and the swim bladder, semicircular canals,
45 and myelinated nerves (24–27). Accurate phylogenies have been crucial for resolving the
46 stepwise evolution of these features (22, 23, 28, 29).

47 The over 1200 species of living cartilaginous fishes (30) last share a common ancestor
48 that diverged from other vertebrates at least 439 million years ago (31) and include a large
49 proportion of unique evolutionary history (32). The early fossil record of cartilaginous
50 vertebrates (*Chondrichthyes*) provides key clues about the origins of living jawed vertebrate
51 diversity (33–41), and the evolution of their varied reproductive modes (42) and massive genome
52 sizes (43–47) has received much attention in the context of understanding major transitions in
53 vertebrate genomics and life history. Yet, we still lack a comprehensive phylogeny of the
54 *Chondrichthyes* based on genomic data. The few studies incorporating genome-wide markers to
55 infer chondrichthyan phylogeny (43, 48, 49) do not sample all of the major orders of sharks,
56 meaning that they do not test the essential disagreement among evolutionary trees generated
57 using mitochondrial (50–53) and legacy nuclear (54–56) markers or morphological characters
58 (57, 58): whether sharks and rays are reciprocally monophyletic.

59 Here, we leverage genome-wide marker data for 48 species representing all major living
60 lineages of chondrichthyans to infer their phylogenetic relationships and timescale of
61 diversification. Using multiple types of genomic markers and legacy nuclear gene data, we
62 provide a robust resolution of chondrichthyan phylogeny with the exception of one critical node:
63 the root of sharks, skates, and rays to the exclusion of chimaeras (*Elasmobranchii*). Phylogenies
64 inferred from ultraconserved elements confidently reject the monophyly of sharks relative to rays
65 and skates and show that six-gilled and frilled sharks in the clade *Hexanchiformes* are the living
66 sister to all other elasmobranchs. However, phylogenies built using single-copy exons support
67 the traditional hypothesis that sharks and rays are reciprocally monophyletic. By examining the
68 proportions of individual genes and sites that support these alternative hypotheses and
69 considering factors such as compositional bias, we demonstrate that exon sequences might be
70 less reliable for inferring deep chondrichthyan relationships, but that the root of sharks is
71 nonetheless a hard phylogenetic problem. Nonetheless, we show that key inferences about the
72 evolution of sharks, including their ancestral ecology, genome size, and tempo of major lineage
73 divergences, remain consistent even when shark paraphyly is considered. In particular, we
74 confirm a Mesozoic diversification of chondrichthyans that included the rapid interordinal
75 diversification of both galeomorph and squalomorph sharks during the Early and Middle Jurassic.
76 These results illuminate the exceptionally ancient diversity contained in living sharks, rectify
77 long-debated scenarios of jaw, genome size, life history, and ecomorphological evolution in
78 chondrichthyans, and provide new clarity on the evolutionary history of one of three major
79 divisions of jawed vertebrates.

80

81 **Results and Discussion.**

82 **A hard phylogenetic problem at the common ancestry of sharks and rays.**

83 Using a total of 349 ultraconserved elements (UCEs) and 840 basic universal single copy
84 orthologs (BUSCOs) extracted from 48 chondrichthyan genomes and six osteichthyan outgroups,
85 we conducted comprehensive phylogenomic analyses of cartilaginous vertebrates. UCEs are
86 highly conserved regions of genomes found across taxa with ancient divergences; targeting
87 UCEs also allows for selection of their more variable flanking regions (59). In contrast, BUSCOs
88 are conserved protein-coding sequences (60). Consequently, targeting BUSCOs and UCEs
89 provides us with two compositionally different sequence datasets with which to analyze and infer
90 chondrichthyan relationships. The resulting phylogenies (Figure 1A, Figure 2; Figures S1-S12)
91 inferred using maximum likelihood and a multispecies coalescent model are congruent across
92 most major clades of contention in *Chondrichthyes*, supporting skates (*Rajiformes*) and torpedo

93 rays (*Torpediniformes*) as the first two successive divergences in rays and skates (*Batoidea*), the
94 monophyly of a clade containing sharks in the orders *Carchariniiformes* and *Lamniformes*, and
95 the monophyly of *Squalomorphii* (dogsharks, angelsharks, sawsharks, and prickly sharks)
96 (Figure 1). Analyses of legacy molecular datasets have resolved the relationships of these
97 lineages in many different ways (32, 43, 44, 50, 55, 56, 61–63), and so our phylogenomic
98 analyses incorporating different genome marker datasets provide consensus regarding key
99 chondrichthyan relationships.

100 Nonetheless, phylogenies inferred from UCEs and BUSCOs consistently resolve
101 alternative topologies for the earliest divergence among sharks, skates, and rays (*Elasmobranchii*)
102 (Figure 1). Phylogenetic analysis of UCEs results in *Hexanchiformes* (represented by
103 *Heptranchias perlo* in our phylogeny) resolved as the sister lineage of all other sharks and rays.
104 The *Squalomorphii*, which includes dogfishes, angelsharks, sawsharks, and pricklysharks (50, 51,
105 55), is resolved with weak node support as the sister to other sharks besides *Hexanchiformes* or
106 outside a clade containing rays and skates (*Batoidea*) and all other sharks (*Galeomorphii*). In
107 contrast, all analyses of the BUSCO dataset resolve a traditional *Squalomorphii* in which
108 *Hexanchiformes* as the earliest diverging lineage (Figure 1A) (32, 50, 51, 56, 61–63).
109 Interrogation of different metrics of node support across analyses shows that the resolution of
110 *Hexanchiformes* as the sister lineage to all other sharks and rays is not the only region of
111 phylogenetic instability; whereas monophyly of all other sharks and rays to the exclusion of
112 *Hexanchiformes* is consistently supported by bootstrap values of 100 and high gene and site
113 concordance factors, the monophyly of the clade consisting of all other sharks (*Galeomorphii* +
114 *Squalomorphii*) is only moderately supported (Figure 1B). In contrast, all phylogenies inferred
115 from BUSCOs strongly infer shark monophyly. Our alternative inferences of shark paraphyly
116 and monophyly are robust to different levels of data completeness (Figure 1B; Figures S1–S12).
117 Bayesian analysis of legacy nuclear sequences sampled for a larger number of chondrichthyan
118 species (including the deeply divergent *Echinorhinus* prickly sharks) resolves sharks as
119 paraphyletic, placing *Heptranchias perlo* as the sister taxon to other squalomorphs with weak
120 node support (posterior = 0.51; Figure S10). Although we were unable to sample *Echinorhinus*
121 in our phylogenomic analyses, previous phylogenies generated using mitochondrial and nuclear
122 markers (32, 50, 55, 61) as well as genome-wide exon markers (64) consistently place
123 *Echinorhinus* in *Squalomorphii* nested within *Squaliformes*, *Squatina*, and *Pristiophoriformes*,
124 which is consistent with our phylogenetic analysis of legacy marker data (Figure S7).

125 Phylogenetic incongruence among different genome-wide datasets has become widely
126 observable across major vertebrate clades such as birds (8–10, 65–72), placental mammals (7,
127 73–75), and teleost fishes (6, 76–79). To further identify sources of support for shark monophyly
128 across our UCE and BUSCO datasets, we examined both the base composition of the underlying
129 sequence data and phylogenetic support across gene trees and sites. Failure to resolve shark
130 monophyly in molecular phylogenetic analyses of legacy nuclear markers has been attributed to
131 GC bias (56), and phylogenetic analyses of other clades using UCEs and BUSCOs have shown
132 that GC bias might limit the capacity of BUSCOs to infer the relationships of deeply divergent
133 species (71). Comparisons of the nucleotide base composition of our datasets shows that the
134 sampled BUSCOs have a considerably (3–6%) higher GC content than sampled UCEs (Figure
135 1C). Second, though BUSCOs have a higher gross number of parsimony informative sites (PIS)
136 than UCEs, they also exhibit a higher degree of PIS variance per sequence alignment (Table 1).
137 Gene and site concordance factors calculated for species trees inferred using BUSCOs also
138 exhibit less linear relationships than those calculated for trees inferred using UCEs (Figure S13).

139 For these reasons, we slightly favor the hypothesis supported using UCEs though acknowledge
140 the initial divergence of elasmobranchs is a hard phylogenetic problem.

141 The phylogeny of sharks that we infer using UCEs would render the terms *Selachii*
142 Gadow 1898 (80) and *Neoselachii* Compagno 1977 (58), used to refer to a monophyletic shark
143 lineage (54, 81), as junior subjective synonyms of *Elasmobranchii* Bonaparte 1838 (82). These
144 results differ considerably from previous studies using molecular data (Figure S7), where
145 *Hexanchiformes* is found to be the oldest-diverging clade in *Squalomorphii* and sharks are
146 monophyletic relative to rays (50, 51, 55, 62). Our inference of paraphyly of sharks is robust to
147 different levels of data completeness (Figure 2A, B; Figures S1-S7), and is congruent with
148 Bayesian analysis of legacy nuclear sequences sampled for a larger number of chondrichthyan
149 species (including the deeply divergent *Echinorhinus* prickly sharks), which fails to resolve
150 sharks as monophyletic and places *Heptranchias perlo* as the sister taxon to other squalomorphs
151 with weak node support (posterior = 0.51; Figure S8). Although we were unable to sample
152 *Echinorhinus* in our phylogenomic analyses, previous phylogenies generated using
153 mitochondrial and nuclear markers (32, 50, 55, 61) as well as genome-wide exon markers (64)
154 consistently place *Echinorhinus* in *Squalomorphii* nested within *Squaliformes*, *Squatina*, and
155 *Pristiophoriformes*, a position consistent with the phylogeny inferred from our analysis of legacy
156 markers (Figure S7).

157 Shark paraphyly was previously proposed on the basis of morphological characters (83,
158 84), a result that was subsequently challenged several times on the basis of molecular
159 phylogenies built using legacy nuclear and mitochondrial sequence data (50, 55, 56, 61–63).
160 Although our analyses of BUSCOs reject the paraphyly of *Squalomorphii* relative to *Batoidea* as
161 found in these analyses of morphological data (83, 84), the phylogenetic resolution of
162 *Hexanchiformes* in analyses of the UCE dataset is consistent with the hypothesis that amphistylic
163 jaw suspension is ancestral for elasmobranchs (85–87). Our results also challenge the hypothesis
164 that the root of *Elasmobranchii* is unresolvable due to the long divergence time between
165 elasmobranchs and holocephalans (56). A previous study of legacy nuclear markers rejected the
166 hypothesis that *Hexanchiformes* is sister to other sharks and *Batoidea* based on the long branch
167 lengths subtending *Elasmobranchii*, despite resolving *Hexanchiformes* in the same position as
168 we do using UCEs (56). A similar argument was put forth with reference to the same problem in
169 a recent preprint using genome-wide loci (88), which suggested that extensive filtering is
170 necessary to prevent long branch attraction, heterogenous evolutionary rates, and GC content
171 bias from inhibiting resolution of shark relationships. This hypothesis is also challenged by the
172 resolution of older or similarly old relationships across the animal Tree of Life using genomic data
173 (1–3, 5), including the resolution of lungfishes and coelacanths as sarcopterygians (15, 89–95),
174 the stepwise divergences of the major ray-finned fish lineages (6, 12, 13, 96–99) among
175 vertebrates. In our node-dated phylogeny, we estimate that crown *Chondrichthyes* appeared
176 383.54 million years ago (Ma) [95% highest posterior density interval (HPD): 353.81, 412.01
177 Ma], *Hexanchiformes* diverged from other sharks and rays 278.09 million years ago 288.26 Ma
178 (95% HPD: 232.86, 344.27 Ma), and all other sharks and rays share a most recent common
179 ancestor 256.35 Ma (95% HPD: 212.24, 312.02 Ma). These results suggest that the crown age of
180 cartilaginous vertebrates is in fact up to 40 million years younger than the age of crown-group
181 bony vertebrates, which are known from fossils as old as the Silurian, approximately 419 million
182 years ago (100–103).

183 Our hypothesis of the timescale chondrichthyan evolution based on the phylogeny
184 inferred from UCEs supports that the interordinal divergences of elasmobranchs largely

185 correspond to a major periods of marine faunal reorganization during the Jurassic (32, 47, 61, 63,
186 104, 105) (Figure 2). The exception to this is *Hexanchiformes*, which we estimate has a stem
187 lineage that extends into the Paleozoic, highlighting this lineage as a priority for conserving
188 ancient chondrichthyan biodiversity (32). Nearly all shark and ray interordinal divergences occur
189 during the Early-Middle Jurassic, including a rapid diversification among shark order-level
190 lineages (Figure 2) including *Carcharhiniformes* (hammerheads, requiem sharks, and catsharks),
191 *Lamniformes* (white sharks, megamouth and basking sharks, and thresher sharks), and
192 *Orectolobiformes* (whale sharks, wobbegong sharks, zebra sharks, and nurse sharks). This period
193 coincided with Mesozoic Marine Revolution, which featured major diversifications of benthic
194 and demersal species, as well as large predators (106–111). Phylogenomic studies of teleost
195 fishes (6) suggest broad interordinal diversification during this time in the marine realm across
196 depth ranges (112, 113). Similarly, transcriptomic data from coleoid cephalopods (114) indicates
197 that the initial diversification of octopuses and squids occurred during the Triassic-Jurassic.
198 Further, this result supports the hypothesis (61, 104) that large-bodied, pelagic sharks appeared
199 in the Jurassic and Early Cretaceous, well after the initial diversification of most marine reptile
200 clades in the earliest Triassic (115–118) with the notable exception of several marine
201 crocodylomorph clades (119–123) and mosasaurs (124–126).

202

203 **The evolution of jaws in sharks and rays and the rise of pelagic planktivores.**

204 The alternative phylogenies of cartilaginous vertebrates that we present warrant a review
205 of the evolution of key anatomical and physiological features in sharks and rays. Ancestrally,
206 sharks and rays (*Elasmobranchii*) are inferred to have either amphistylic jaw suspension,
207 wherein the mandibular arch is braced by the hyomandibula and there is a two-point suspension
208 of the upper jaw-formed by the palatoquadrate-to the chondrocranium, or autodiastyly, where an
209 additional ethmoid articulation forms a three-point suspension system (86, 87, 127, 128). Sharks
210 in the clade *Hexanchiformes* are unique among living species in retaining amphistylic jaw
211 suspension, and have also partially developed orbitostyly, where the palatoquadrate is also
212 anchored to the orbital (86). These modifications to jaw suspension in sharks and rays modify the
213 mobility of the jaws. For example, rays and skates have highly mobile euhylostyly jaws that
214 articulate with the chondrocranium solely via the hyomandibula (87).

215 Hypotheses of shark phylogeny that united *Hexanchiformes* with *Squalomorphii* imply
216 that species in the former clade represent in part a retained amphistylic condition likely found in
217 the ancestral elasmobranch but also acquired features of orbitostyly condition found in lineages
218 of squalomorphs (Figure 1) (83, 84, 86, 87, 128). Our phylogenomic analyses of UCEs, which
219 infer that *Hexanchiformes* is the sister lineage of all other elasmobranchs, imply that the
220 morphology of the jaw articulation in this clade represents the retention of the plesiomorphic
221 condition in elasmobranchs (87). This result consequently suggests that the modified amphistyly
222 of hexanchiform sharks represents the retention of the condition seen in many [but not all, see
223 (38)] early-diverging elasmobranchs, such as the symmoriform pan-holocephalan (36, 129)
224 †*Cladoselache* (87) and the pan-elasmobranch †*Phoebodus* (34).

225 Because we infer a Paleozoic origin for *Hexanchiformes*, it does appear that this deep-
226 water lineage of sharks represents a survivor of ancient Paleozoic elasmobranch diversity.
227 Previous studies that estimated the divergence time of *Hexanchiformes* from other
228 elasmobranchs inferred a Triassic age owing to the placement of this clade within *Squalomorphii*
229 (32, 47, 61). However, the estimated total clade age of *Hexanchiformes* in our phylogeny is
230 younger than Devonian chondrichthyan teeth with controversial phylogenetic affinities that are

231 somewhat similar to living hexanchiforms (130), supporting the hypothesis that these Devonian
232 fossils represent species that converged with living hexanchiforms in dental morphology (131).
233 Our time-calibrated phylogeny of sharks also does not exclude the possibility that the enigmatic
234 of Permian-Jurassic †*Synechodontiformes*—variously considered a monophyletic (132, 133) or
235 paraphyletic (81) group of early-diverging crown or stem-group sharks with dental similarities to
236 some hexanchiforms (134)—are members of the hexanchiform total clade, on the stem of the
237 clade containing all other elasmobranchs, or on the stem of *Elasmobranchii*.

238 Our phylogenomic analyses also support post-Cretaceous origins for specialized species
239 of living pelagic sharks and rays (135). The origins of filter feeding in living lineages of sharks
240 and rays is of great interest because, along with the far more recently diversified baleen whales,
241 the four major lineages of planktivorous elasmobranchs are the only other large-bodied filter-
242 feeding marine vertebrates. However, a variety of lineages, including Jurassic-Cretaceous
243 pachyormid fishes (136–138), Cretaceous elasmobranchs with possible stem-lamniform affinities
244 (135), the Devonian ‘placoderm’ stem-gnathostome †*Titanichthys* (139), and Cambrian-
245 Ordovician radiodont stem-arthropods (140, 141) have independently exploited the giant
246 planktivore niche over 500 million years of Earth History. Our time-calibrated phylogeny
247 (Figure 2) places the origination of three (manta rays, *Mobulidae*; Whale Shark, *Rhincodon typus*;
248 Basking Shark, *Cetorhinus maximus*) of the four living lineages of giant, pelagic (Figure 3A)
249 planktivorous chondrichthyans after the Cretaceous-Paleogene boundary and following the
250 extinction of giant filter-feeding fishes and ray-like lamniforms (135, 136); this result is
251 consistent with the fossil record (135–137, 142). We confirm that least two of these lineages, the
252 *Mobula* rays and the Whale Shark, evolved among ancestrally benthopelagic, rather than pelagic,
253 clades, based on ancestral state reconstructions on the time-calibrated phylogeny (Figure 3A).
254 The Cenozoic age of living planktivore sharks and rays inferred using our UCE dataset are
255 congruent with the hypothesis that plankton turnover and extinction at the Cretaceous-Paleogene
256 boundary may have contributed to the faunal turnover of giant filter-feeding vertebrates (135,
257 136, 143). Although genomic data for Megamouth Shark *Megachasma pelagios* is unavailable,
258 our Bayesian phylogeny of elasmobranchs based on *rag1* sequences, which places this taxon
259 sister to sand sharks (*Odontaspis ferox*), supports the inference (144, 145) that this species
260 independently acquired filter feeding.

261 262 **Ecology, life history, and genomic evolution of sharks and rays.**

263 *Elasmobranchii* is notable for the apparent convergent evolution of multiple modes of
264 viviparity within the clade (42, 47, 146–149). Our ancestral state reconstructions of parity mode
265 using the phylogeny of *Chondrichthyes* inferred using UCEs (Figure 3B) indicates a higher
266 degree of uncertainty associated with the ancestral parity mode of cartilaginous fishes than
267 inferred in previous studies, which reconstruct oviparity as the ancestral state (42, 150–152). As
268 in previous studies, we find a high degree of uncertainty underlies inferred ancestral parity states
269 in sharks (42, 150), which is likely driven by the presence of both oviparous and viviparous
270 species in several orders (Figure 3B). Indeed, analyses of larger taxonomic samples of
271 chondrichthyans using phylogenies inferred from molecular sequence data have generally found
272 that oviparity precedes viviparity and reversions to oviparity are rare (150–152). Given that
273 multiple lineages of stem-gnathostome ‘placoderms’ (153, 154) and some stem-holocephalans
274 (155) were viviparous, our study raises the intriguing possibility of complex parity mode
275 evolution proximal to the common ancestor of crown gnathostomes (Figure 3B). Notably, we
276 also find that all planktivorous lineages ancestrally possessed aplacental viviparity (Figure 3B)

277 (42, 61). Given recent interest in how paedomorphosis (156) and increased maternal investment
278 (42, 151, 156) might be associated with adaptations for filter-feeding and body size increases,
279 respectively, in sharks and rays, our findings are intriguing for supporting the existence of a
280 common developmental mode in these large pelagic filter-feeding lineages.

281 Our understanding of chondrichthyan genome evolution has been hampered by the
282 massive genomes of elasmobranchs (46) which outside of lungfishes (89, 90) and lissamphibians
283 (157–160) are the largest known vertebrate genomes (43, 47, 48). The evolution of genome size
284 in sharks, skates, rays, and other vertebrates has been related to life history and metabolic
285 evolution (47, 158, 160). Using measurements of published genome sequence lengths (In-
286 gigabase pairs) and genome weight (47), we reconstructed ancestral genome size across
287 *Chondrichthyes* to infer the timescale of genomic expansion in this clade. Our reconstruction of
288 genome size evolution infers a single increase in genome size at the common ancestor of
289 *Elasmobranchii* (Figure 4A) and implies high subclade disparity in genome size characterized
290 early crown chondrichthyan evolution (Figure 4B). Observed disparity in genome size from the
291 start of the Mesozoic to the present is not outside the expectations of Brownian motion (Figure
292 4B). A recent study that examined shark genome size evolution (as measured in picograms)
293 found evidence for an initial increase in genome size at the common ancestor of sharks
294 (monophyletic in their reference tree) followed by substantial, parallel expansions in
295 *Heterodontus* and all squalomorphs except *Hexanchiformes* [figure 1 in (47)]. In contrast,
296 ancestral state reconstructions suggest that the comparatively small genome sizes of
297 hexanchiform sharks reflect their early divergence from other sharks, rays, and skates, rather
298 than being a secondary reduction (Figure 4A; Figure S9).

299

300 **Conclusions.**

301 Using newly-assembled datasets of UCEs and BUSCOs from 38 chondrichthyan
302 genomes spanning the major shark, ray, and skate clades, we are able to resolve shark
303 relationships with the exception of the placement of *Hexanchiformes*, which is placed
304 alternatively as the sister to all other shark lineages or as the deepest divergence in
305 *Squalomorphii* depending on the dataset used (Figure 1, Figure 2). Although the resolution of
306 this lineage is a hard phylogenetic problem, our analyses suggest that analyses of BUSCOs,
307 which are exons, might be affected by compositional biases. Previous studies of avian (66, 71),
308 cichlid (79), and frog (161) phylogenetics have also found that UCEs outperform exons and are
309 more robust to data subsampling strategy. The phylogenomic hypothesis of shark evolution
310 wherein traditional sharks are paraphyletic (Figure 1, Figure 2) suggests that the cranial anatomy
311 and genome sizes of *Hexanchiformes* are reflective of their deeply divergent phylogenetic
312 position rather than secondary reversions following modifications to jaw articulation and genome
313 size expansion at the base of *Elasmobranchii* (47, 86, 87). Our time-calibrated phylogeny
314 supports a Jurassic diversification of most sharks and a Cretaceous-Paleogene diversification of
315 rays, skates, and relatives (Figure 2). We also infer post-Cretaceous origins of living giant
316 planktivore chondrichthyans (Figure 2; Figure 3A), supporting the hypothesis that these taxa
317 occupied that niche following the extinction of Mesozoic filter-feeding teleosts and
318 chondrichthyans (135, 136). By clarifying where phylogenetic uncertainty remains in the
319 relationships of one of the two major divisions of crown-group jawed vertebrates, we illuminate
320 the unexpectedly ancient evolutionary history of some chondrichthyans that are now under threat
321 of extinction due to the current anthropogenic biodiversity crisis (32).

322

323 **Methods.**

324 **Taxonomy.**

325 In this manuscript, we follow the taxonomic conventions of phylogenetic rank-free taxonomy
326 formalized in the PhyloCode (162), which has recently been applied to both ray-finned fishes
327 (*Actinopterygii*)(163–165) and chimaeras and ratfishes (*Holocephali*)(166). In practice, this
328 means following emerging conventions for italicizing clade names (167), using the prefix pan- to
329 refer to total clades and stem lineages of crown clades, and finally removing redundant clade
330 names. In this manuscript, for example, we do not use the traditional crown ‘orders’ for Bramble
331 Sharks (*Echinorhiniformes*) and Angel Sharks (*Squatiniiformes*), since each of these clades is
332 represented by one living genus each (*Echinorhinus* and *Squatina*). Thus, *Echinorhiniformes* is
333 redundant with *Echinorhinus*, and *Squatiniiformes* with *Squatina* according to the PhyloCode.

334

335 **UCE Sequence Dataset Assembly.**

336 In order to leverage genome-scale data to analyze chondrichthyan relationships, we used phyluce
337 1.7.3 (168) to extract ultraconserved elements from 48 published chondrichthyan genomes and
338 six outgroups, align them, and produce 75% and 90% complete matrices to assess the effect of
339 data completeness on inference of shark interrelationships. We used the 5k vertebrate
340 ultraconserved element probe set (59). Following UCE extraction and alignment creation, we
341 used CIAAlign (169) to visualize and prune chimaeric UCE sequence alignments. Our final set
342 consisted of 356 ultraconserved element sequences for 48 chondrichthyans and six osteichthyan
343 outgroups: *Homo sapiens*, *Latimeria chalumnae*, *Polypterus senegalus*, *Scleropages formosus*,
344 *Amia ocellicauda* (labeled *Amia calva* on Genbank; S. David pers. comm.), and *Lepisosteus*
345 *oculatus*. We conducted all UCE dataset assembly steps on the Yale high-performance
346 computing cluster McCleary.

347

348 **BUSCO Sequence Dataset Assembly.** In order to assess how different genomic datasets might
349 affect inference of chondrichthyan relationships (170), we used Augustus in BUSCO 5.8.3 (171,
350 172) to locate and extract 954 genes conserved across metazoans using the metazoa_odb10
351 dataset, following a previous study (49). Several genomes were not of sufficient quality for
352 BUSCO genes to be found, so only a total of 45 genomes were used. We collected and aligned
353 the output nucleotide sequences using MAFFT (173) and then used commands in phyluce-1.7.3
354 and CIAAlign to reduce the alignment to 75% and 90% complete matrices and filter chimaeric
355 alignments. Our final 75% complete set consisted of 840 BUSCO sequences for 39
356 chondrichthyans and 6 osteichthyan outgroups, and our 90% complete set consisted of 483
357 BUSCO sequences for the same species. We conducted all BUSCO dataset assembly steps on
358 the Yale high-performance computing cluster McCleary.

359

360 **Legacy Nuclear Gene Dataset Assembly and Analysis.** To exploit the availability of legacy
361 nuclear gene sequence data for a larger sample of chondrichthyans, we aligned all sequences of
362 recombination activating gene 1 (*rag1*) available for 161 chondrichthyans on the NCBI
363 repository GenBank, then ran an uncalibrated Bayesian phylogenetic analysis using MrBayes
364 3.2.7 (174). For this analysis, we partitioned the sequences by codon position, used an
365 HKY+I+G model, and ran four chains over 10 million generations sampling every thousand
366 generations. Finally, we checked for convergence of the posteriors using Tracer 1.7.1 (175) and
367 summarized the posterior tree sets in a single maximum clade credibility tree.

368

369 **Maximum Likelihood Phylogenetic Analysis of Genomic Data.**

370 We conducted maximum likelihood phylogenetic analyses in IQ-TREE2 (176, 177) on the
371 concatenated 75% and 90% UCE and BUSCO sequence datasets. Concatenated datasets were
372 alternately treated as a single partition or multiple partitions; in the latter case, we used
373 PartitionFinder 2 (178) to select partitioning schemes. Gene trees were inferred from each UCE
374 locus using IQ-TREE2, models of nucleotide evolution were chosen using ModelFinder as
375 implemented in IQ-TREE2 (179). Node support was assessed using 1000 ultrafast bootstrap
376 replicates. We used the individual gene trees to generate a species tree using the coalescent
377 model implemented in ASTRAL-III (180). Next, we explored site-wide and gene-wide nodal
378 support for the inferred phylogenies using gene and site concordance factors, which measure the
379 number of decisive gene trees and sites that support a given topology in an input tree (here, the
380 single partition concatenated phylogeny) (181). Using custom scripts in ggplot2
381 (https://www.robertlanfear.com/blog/files/concordance_factors.html), we plotted concordance
382 factors against one another and branch lengths in the maximum likelihood phylogeny. Next, we
383 used commands in phyluce-1.7.3 to collect information on nucleotide base content and
384 parsimony informative site counts for both the BUSCO and UCE datasets at varying levels of
385 completeness. All phylogenetic analyses were conducted on the Yale high-performance
386 computing cluster McCleary.

387

388 **Bayesian Time-Calibration.**

389 We inferred a time-calibrated phylogeny of *Chondrichthyes* using a Bayesian node-dating
390 approach implemented in BEAST 2.6.6 (182, 183) for three sets of 50 UCEs (owing to their
391 higher taxon sampling) from the 90% complete matrix. We applied a stringent set of criteria to
392 choose a set of 14 fossil calibrations (53, 105) to calibrate the phylogeny, as the fossil record of
393 chondrichthyans includes numerous occurrences based on fragmentary or isolated fossils that
394 may simply represent species that converged, for example, on the dental anatomy of living
395 species. As such, we searched for holomorphic fossils that are universally agreed to represent
396 members of the relevant crown clades and have been placed in phylogenetic analyses of
397 morphological characters (Supplementary Text). The final fossil calibration dataset included 12
398 species based on holomorphic specimens and two tooth taxa commonly used in time calibration
399 of chondrichthyan phylogeny (63, 105).

400 For all three UCE sets, we constructed input xml files in BEAUTi 2.6.7 (182, 183). We
401 used a general-time-reversible model of molecular sequence evolution with a gamma site model,
402 a relaxed log-normal clock model, and the fossilized birth-death branching model as
403 implemented in BEAST2 (184). We set the origin prior to 443.8 Ma, the Ordovician-Silurian
404 boundary, as crown gnathostomes are known up to, but not before, the start of the Silurian (31,
405 31, 185). The bounds on the origin priors were 439.0 Ma, the age of the oldest anatomically
406 well-characterized crown-group gnathostome (185), and 509.0, the minimum age of the stem-
407 vertebrate-bearing (186) Burgess-Shale. We set the diversification rate to 0.018, which is the
408 mean diversification rate estimate according to the formula of (187) given 1489 living
409 chondrichthyan species (188) and an origin of 443.8 Ma, with bounds of 0.00 and 1.00. Next, we
410 set rho, the proportion of living species sampled, to 0.032 (48/1489). We constrained the
411 topology to the ASTRAL-III phylogeny generated from analysis of the 90% complete UCE
412 matrix, ran three independent BEAST2 chains over 600 million generations with a 50 million
413 generation pre-burnin on the Yale high performance computing cluster McCleary, and checked
414 for convergence of the posteriors and effective sample size values over 200 in Tracer v. 1.7.1

415 (175). After combining the 9 tree sets in LogCombiner 2.6.7 (182) with 75% burnin sampling
416 every 5000 generations, we annotated the ASTRAL-III target tree with median node height
417 values in TreeAnnotator v. 2.6.6 (182).

418

419 **Ancestral State Reconstructions and Disparity Through Time.**

420 We compiled data on shark habitat preference (pelagic/benthopelagic/benthic)(61) and
421 parity mode from Fishbase and previous studies (42, 150) and conducted ancestral state
422 reconstructions on the Bayesian time-calibrated phylogeny using stochastic mapping over 1000
423 simulations using the R package phytools (189, 190). For our analyses of genome sizes, we
424 collected data on genome sequence length in gigabase pairs and chromosome number from
425 Genbank using given GenBank lengths and data on genome size in picograms from a previous
426 study (47) and the Animal Genome Size Database (<https://www.genomesize.com/>; chromosome
427 numbers were also collected from this database if needed). If other species in a genus included in
428 our phylogeny were represented in the Animal Genome Size Database, we took the mean
429 genome size value for these species as a proxy for genome size of the species included in our tree.
430 In one case, we reduced our sample of *Mobula* to a single tip to institute this approach. Because
431 no data is available on total genome size in picograms for *Heptrachias perlo*, we took the
432 average of genome sizes reported for members of *Hexanchiformes* and inputted the value for that
433 taxon, which represents this whole clade in our tree. Next, we used scripts in the R packages
434 phytools and geiger (191) to fit four models of evolution (Brownian Motion, Ornstein-Uhlenbeck,
435 White Noise, and Early Burst) on the log-transformed genome sequence length and size data,
436 produce traitgrams scaled by these measurements, and produce disparity-through-time plots of
437 genome length and size over time.

438

439 **Acknowledgements.**

440 We thank members of the Near Lab for discussions related to this manuscript. We also thank the
441 editor and reviewers for their helpful comments.

442

443 **Funding.**

444 CDB is supported by the Yale Training Program in Genetics. TJN is supported by the National
445 Science Foundation (DEB 2508641) and the Bingham Oceanographic Fund maintained by the
446 Yale Peabody Museum, Yale University.

447

448 **References.**

- 449 1. D. T. Schultz, *et al.*, Ancient gene linkages support ctenophores as sister to other animals.
450 *Nature* **618**, 110–117 (2023).
- 451 2. C. W. Dunn, G. Giribet, G. D. Edgecombe, A. Hejnol, Animal Phylogeny and Its Evolutionary
452 Implications*. *Annual Review of Ecology, Evolution, and Systematics* **45**, 371–395 (2014).
- 453 3. C. W. Dunn, *et al.*, Broad phylogenomic sampling improves resolution of the animal tree of
454 life. *Nature* **452**, 745–749 (2008).
- 455 4. C. E. Laumer, *et al.*, Revisiting metazoan phylogeny with genomic sampling of all phyla.
456 *Proceedings of the Royal Society B: Biological Sciences* **286**, 20190831 (2019).

- 457 5. M. J. Telford, G. E. Budd, H. Philippe, Phylogenomic Insights into Animal Evolution. *Current*
458 *Biology* **25**, R876–R887 (2015).
- 459 6. L. C. Hughes, *et al.*, Comprehensive phylogeny of ray-finned fishes (Actinopterygii) based
460 on transcriptomic and genomic data. *Proc Natl Acad Sci U S A* **115**, 6249–6254 (2018).
- 461 7. N. M. Foley, *et al.*, A genomic timescale for placental mammal evolution. *Science* **380**,
462 eabl8189 (2023).
- 463 8. E. D. Jarvis, *et al.*, Whole-genome analyses resolve early branches in the tree of life of
464 modern birds. *Science* **346**, 1320–1331 (2014).
- 465 9. R. O. Prum, *et al.*, A comprehensive phylogeny of birds (Aves) using targeted next-
466 generation DNA sequencing. *Nature* **526**, 569–573 (2015).
- 467 10. S. J. Hackett, *et al.*, A Phylogenomic Study of Birds Reveals Their Evolutionary History.
468 *Science* **320**, 1763–1768 (2008).
- 469 11. F. Delsuc, H. Brinkmann, D. Chourrout, H. Philippe, Tunicates and not cephalochordates are
470 the closest living relatives of vertebrates. *Nature* **439**, 965–968 (2006).
- 471 12. A. W. Thompson, *et al.*, The bowfin genome illuminates the developmental evolution of
472 ray-finned fishes. *Nat Genet* **53**, 1373–1384 (2021).
- 473 13. E. Parey, *et al.*, Genome structures resolve the early diversification of teleost fishes. *Science*
474 **379**, 572–575 (2023).
- 475 14. F. T. Burbrink, *et al.*, Interrogating Genomic-Scale Data for Squamata (Lizards, Snakes, and
476 Amphisbaenians) Shows no Support for Key Traditional Morphological Relationships.
477 *Systematic Biology* **69**, 502–520 (2020).
- 478 15. P. M. Hime, *et al.*, Phylogenomics Reveals Ancient Gene Tree Discordance in the Amphibian
479 Tree of Life. *Syst Biol* **70**, 49–66 (2020).
- 480 16. T. J. Near, Conflict and resolution between phylogenies inferred from molecular and
481 phenotypic data sets for hagfish, lampreys, and gnathostomes. *J Exp Zool B Mol Dev Evol*
482 **312**, 749–761 (2009).
- 483 17. T. Miyashita, *et al.*, Hagfish from the Cretaceous Tethys Sea and a reconciliation of the
484 morphological–molecular conflict in early vertebrate phylogeny. *Proceedings of the*
485 *National Academy of Sciences* **116**, 2146–2151 (2019).
- 486 18. D. Bardack, “Relationships of Living and Fossil Hagfishes” in *The Biology of Hagfishes*, J. M.
487 Jørgensen, J. P. Lomholt, R. E. Weber, H. Malte, Eds. (Springer Netherlands, 1998), pp. 3–
488 14.

- 489 19. P. C. Donoghue, P. L. Forey, R. J. Aldridge, Conodont affinity and chordate phylogeny. *Biol*
490 *Rev Camb Philos Soc* **75**, 191–251 (2000).
- 491 20. M. W. Hardisty, *Biology of the Cyclostomes* (Springer US, 1979).
- 492 21. S. Kuraku, S. Kuratani, Time scale for cyclostome evolution inferred with a phylogenetic
493 diagnosis of hagfish and lamprey cDNA sequences. *Zoolog Sci* **23**, 1053–1064 (2006).
- 494 22. F. Marlétaz, *et al.*, The hagfish genome and the evolution of vertebrates. *bioRxiv*
495 2023.04.17.537254 (2023). <https://doi.org/10.1101/2023.04.17.537254>.
- 496 23. D. Yu, *et al.*, Hagfish genome elucidates vertebrate whole-genome duplication events and
497 their evolutionary consequences. *Nat Ecol Evol* **8**, 519–535 (2024).
- 498 24. J. S. Anderson, H.-D. Sues, *Major Transitions in Vertebrate Evolution* (Indiana University
499 Press, 2007).
- 500 25. M. I. Coates, The Evolution of Paired Fins. *Theory in Biosciences* **122**, 266–287 (2003).
- 501 26. B. Fritzsche, K. W. Beisel, Evolution and development of the vertebrate ear. *Brain Res Bull* **55**,
502 711–721 (2001).
- 503 27. B. Zalc, The acquisition of myelin: An evolutionary perspective. *Brain Research* **1641**, 4–10
504 (2016).
- 505 28. S. Higuchi, *et al.*, Inner ear development in cyclostomes and evolution of the vertebrate
506 semicircular canals. *Nature* **565**, 347–350 (2019).
- 507 29. Y. Nakatani, *et al.*, Reconstruction of proto-vertebrate, proto-cyclostome and proto-
508 gnathostome genomes provides new insights into early vertebrate evolution. *Nat*
509 *Commun* **12**, 4489 (2021).
- 510 30. R. Fricke, W. N. Eschmeyer, R. V. D. Laan, ESCHMEYER'S CATALOG OF FISHES: GENERA,
511 SPECIES, REFERENCES. *Electronic Version*. Available at:
512 <http://researcharchive.calacademy.org/research/ichthyology/catalog/fishcatmain.asp>
513 [Accessed 30 December 2024].
- 514 31. Y. Zhu, *et al.*, The oldest complete jawed vertebrates from the early Silurian of China.
515 *Nature* **609**, 954–958 (2022).
- 516 32. R. W. Stein, *et al.*, Global priorities for conserving the evolutionary history of sharks, rays
517 and chimaeras. *Nat Ecol Evol* **2**, 288–298 (2018).
- 518 33. B. King, T. Qiao, M. S. Y. Lee, M. Zhu, J. A. Long, Bayesian Morphological Clock Methods
519 Resurrect Placoderm Monophyly and Reveal Rapid Early Evolution in Jawed Vertebrates.
520 *Systematic Biology* **66**, 499–516 (2017).

- 521 34. L. Frey, *et al.*, The early elasmobranch Phoebodus: phylogenetic relationships,
522 ecomorphology and a new time-scale for shark evolution. *Proceedings of the Royal*
523 *Society B: Biological Sciences* **286**, 20191336 (2019).
- 524 35. M. I. Coates, K. Tietjen, The neurocranium of the Lower Carboniferous shark. *Earth and*
525 *Environmental Science Transactions of The Royal Society of Edinburgh* **108**, 19–35 (2017).
- 526 36. M. I. Coates, R. W. Gess, J. A. Finarelli, K. E. Criswell, K. Tietjen, A symmoriiform
527 chondrichthyan braincase and the origin of chimaeroid fishes. *Nature* **541**, 208–211
528 (2017).
- 529 37. M. I. Coates, *et al.*, An early chondrichthyan and the evolutionary assembly of a shark body
530 plan. *Proceedings of the Royal Society B: Biological Sciences* **285**, 20172418 (2018).
- 531 38. M. I. Coates, K. Tietjen, A. M. Olsen, J. A. Finarelli, High-performance suction feeding in an
532 early elasmobranch. *Sci Adv* **5**, eaax2742 (2019).
- 533 39. A. Pradel, J. G. Maisey, P. Tafforeau, R. H. Mapes, J. Mallatt, A Palaeozoic shark with
534 osteichthyan-like branchial arches. *Nature* **509**, 608–611 (2014).
- 535 40. A. Pradel, *et al.*, Skull and brain of a 300-million-year-old chimaeroid fish revealed by
536 synchrotron holotomography. *Proceedings of the National Academy of Sciences* **106**,
537 5224–5228 (2009).
- 538 41. R. P. Dearden, A. Herrel, A. Pradel, Evidence for high-performance suction feeding in the
539 Pennsylvanian stem-group holocephalan Iniopera. *Proceedings of the National Academy*
540 *of Sciences* **120**, e2207854119 (2023).
- 541 42. G. Katona, *et al.*, Evolution of reproductive modes in sharks and rays. *Journal of*
542 *Evolutionary Biology* **36**, 1630–1640 (2023).
- 543 43. Y. Hara, *et al.*, Shark genomes provide insights into elasmobranch evolution and the origin
544 of vertebrates. *Nat Ecol Evol* **2**, 1761–1771 (2018).
- 545 44. N. J. Marra, *et al.*, White shark genome reveals ancient elasmobranch adaptations
546 associated with wound healing and the maintenance of genome stability. *Proceedings of*
547 *the National Academy of Sciences* **116**, 4446–4455 (2019).
- 548 45. M. Tan, *et al.*, The whale shark genome reveals patterns of vertebrate gene family
549 evolution. *eLife* **10**, e65394 (2021).
- 550 46. B. Venkatesh, *et al.*, Elephant shark genome provides unique insights into gnathostome
551 evolution. *Nature* **505**, 174–179 (2014).
- 552 47. M. Torralba Sáez, M. Hofreiter, N. Straube, Shark genome size evolution and its relationship
553 with cellular, life-history, ecological, and diversity traits. *Sci Rep* **14**, 8909 (2024).

- 554 48. J. Wu, *et al.*, Comparative genomics illuminates karyotype and sex chromosome evolution
555 of sharks. *Cell Genomics* **4** (2024).
- 556 49. S. Xu, R. Zhao, S. Cai, P. Li, Z. Han, Application of genomic markers generated for ray-finned
557 fishes in chondrichthyan Phylogenomics. *Org Divers Evol* **23**, 1005–1012 (2023).
- 558 50. G. J. P. Naylor, *et al.*, “Elasmobranch Phylogeny: A Mitochondrial Estimate Based on 595
559 Species” in *Biology of Sharks and Their Relatives*, 2nd Ed., (CRC Press, 2012).
- 560 51. C. R. L. Amaral, F. Pereira, D. A. Silva, A. Amorim, E. F. de Carvalho, The mitogenomic
561 phylogeny of the Elasmobranchii (Chondrichthyes). *Mitochondrial DNA Part A* **29**, 867–
562 878 (2018).
- 563 52. (PDF) Elasmobranch Phylogeny. *ResearchGate*. Available at:
564 https://www.researchgate.net/publication/289995314_Elasmobranch_Phylogeny
565 [Accessed 11 November 2024].
- 566 53. J. G. Inoue, *et al.*, Evolutionary Origin and Phylogeny of the Modern Holocephalans
567 (Chondrichthyes: Chimaeriformes): A Mitogenomic Perspective. *Molecular Biology and*
568 *Evolution* **27**, 2576–2586 (2010).
- 569 54. J. Maisey, Mesozoic elasmobranchs, neoselachian phylogeny and the rise of modern
570 elasmobranch diversity. *Mesozoic fishes* (2004).
- 571 55. X. Vélez-Zuazo, I. Agnarsson, Shark tales: A molecular species-level phylogeny of sharks
572 (Selachimorpha, Chondrichthyes). *Molecular Phylogenetics and Evolution* **58**, 207–217
573 (2011).
- 574 56. C. Li, K. A. Matthes-Rosana, M. Garcia, G. J. P. Naylor, Phylogenetics of Chondrichthyes and
575 the problem of rooting phylogenies with distant outgroups. *Molecular Phylogenetics and*
576 *Evolution* **63**, 365–373 (2012).
- 577 57. J. Maisey, Phylogenetic relationships of the Late Jurassic shark *Protospinax Woodward*
578 *1919* (Chondrichthyes: Elasmobranchii). *Mesozoic Fishes: Systematics and Paleoecology*.
579 *Verlag Dr Friedrich Pfeil, Munich* (1996).
- 580 58. L. J. V. Compagno, Phyletic Relationships of Living Sharks and Rays. *American Zoologist* **17**,
581 303–322 (1977).
- 582 59. B. C. Faircloth, *et al.*, Ultraconserved elements anchor thousands of genetic markers
583 spanning multiple evolutionary timescales. *Syst Biol* **61**, 717–726 (2012).
- 584 60. R. M. Waterhouse, *et al.*, BUSCO Applications from Quality Assessments to Gene Prediction
585 and Phylogenomics. *Mol Biol Evol* **35**, 543–548 (2018).

- 586 61. A. F. P. Marion, F. L. Condamine, G. Guinot, Sequential trait evolution did not drive deep-
587 time diversification in sharks. *Evolution* **78**, 1405–1425 (2024).
- 588 62. G. J. P. Naylor, J. A. Ryburn, O. Fedrigo, J. A. López, “Phylogenetic Relationships among the
589 Major Lineages of Modern Elasmobranchs” in *Reproductive Biology and Phylogeny of*
590 *Chondrichthyes*, (CRC Press, 2005).
- 591 63. N. C. Aschliman, *et al.*, Body plan convergence in the evolution of skates and rays
592 (Chondrichthyes: Batoidea). *Molecular Phylogenetics and Evolution* **63**, 28–42 (2012).
- 593 64. N. Straube, C. Li, J. M. Claes, S. Corrigan, G. J. P. Naylor, Molecular phylogeny of
594 Squaliformes and first occurrence of bioluminescence in sharks. *BMC Evolutionary*
595 *Biology* **15**, 162 (2015).
- 596 65. S. Reddy, *et al.*, Why Do Phylogenomic Data Sets Yield Conflicting Trees? Data Type
597 Influences the Avian Tree of Life more than Taxon Sampling. *Systematic Biology* **66**, 857–
598 879 (2017).
- 599 66. J. Stiller, *et al.*, Complexity of avian evolution revealed by family-level genomes. *Nature* 1–3
600 (2024). <https://doi.org/10.1038/s41586-024-07323-1>.
- 601 67. S. Mirarab, *et al.*, A region of suppressed recombination misleads neoavian phylogenomics.
602 *Proceedings of the National Academy of Sciences* **121**, e2319506121 (2024).
- 603 68. H. Kuhl, *et al.*, An Unbiased Molecular Approach Using 3′-UTRs Resolves the Avian Family-
604 Level Tree of Life. *Molecular Biology and Evolution* **38**, 108–127 (2021).
- 605 69. R. T. Kimball, *et al.*, A Phylogenomic Supertree of Birds. *Diversity* **11**, 109 (2019).
- 606 70. J. S. Berv, *et al.*, Genome and life-history evolution link bird diversification to the end-
607 Cretaceous mass extinction. *Science Advances* **10**, eadp0114 (2024).
- 608 71. L. J. Musher, *et al.*, Whole-genome phylogenomics of the tinamous (Aves: Tinamidae):
609 comparing gene tree estimation error between BUSCOs and UCEs illuminates rapid
610 divergence with introgression. [Preprint] (2024). Available at:
611 <https://www.biorxiv.org/content/10.1101/2024.01.22.576737v2> [Accessed 8 September
612 2025].
- 613 72. E. L. Braun, *et al.*, Testing the mettle of METAL: A comparison of phylogenomic methods
614 using a challenging but well-resolved phylogeny. [Preprint] (2024). Available at:
615 <https://www.biorxiv.org/content/10.1101/2024.02.28.582627v2> [Accessed 8 September
616 2025].
- 617 73. J. E. Tarver, *et al.*, The Interrelationships of Placental Mammals and the Limits of
618 Phylogenetic Inference. *Genome Biology and Evolution* **8**, 330–344 (2016).

- 619 74. M. dos Reis, *et al.*, Phylogenomic datasets provide both precision and accuracy in
620 estimating the timescale of placental mammal phylogeny. *Proc Biol Sci* **279**, 3491–3500
621 (2012).
- 622 75. J. A. Esselstyn, C. H. Oliveros, M. T. Swanson, B. C. Faircloth, Investigating Difficult Nodes in
623 the Placental Mammal Tree with Expanded Taxon Sampling and Thousands of
624 Ultraconserved Elements. *Genome Biology and Evolution* **9**, 2308–2321 (2017).
- 625 76. A. Ghezelayagh, *et al.*, Prolonged morphological expansion of spiny-rayed fishes following
626 the end-Cretaceous. *Nat Ecol Evol* **6**, 1211–1220 (2022).
- 627 77. F. Melendez-Vazquez, *et al.*, Ecological interactions and genomic innovation fueled the
628 evolution of ray-finned fish endothermy. *Science Advances* **11**, eads8488 (2025).
- 629 78. M. E. Alfaro, *et al.*, Explosive diversification of marine fishes at the Cretaceous–Palaeogene
630 boundary. *Nat Ecol Evol* **2**, 688–696 (2018).
- 631 79. F. Alda, W. B. Ludt, D. J. Elías, C. D. McMahan, P. Chakrabarty, Comparing Ultraconserved
632 Elements and Exons for Phylogenomic Analyses of Middle American Cichlids: When Data
633 Agree to Disagree. *Genome Biology and Evolution* **13**, evab161 (2021).
- 634 80. H. Gadow, *A classification of Vertebrata, recent and extinct* (London, 1898).
- 635 81. J. G. Maisey, What is an ‘elasmobranch’? The impact of palaeontology in understanding
636 elasmobranch phylogeny and evolution. *Journal of Fish Biology* **80**, 918–951 (2012).
- 637 82. C. L. Bonaparte, *Selachorum tabula analytica* (1839).
- 638 83. S. Shirai, Phylogenetic interrelationships of neoselachians (Chondrichthyes: Euselachii).
639 *Interrelationships of fishes* 9–34 (1996).
- 640 84. M. R. D. Carvalho, Higher-Level Elasmobranch Phylogeny, Basal Squalians, and Paraphyly.
641 *Interrelationships of Fishes* 35–62 (1996). [https://doi.org/10.1016/b978-012670950-](https://doi.org/10.1016/b978-012670950-6/50004-7)
642 [6/50004-7](https://doi.org/10.1016/b978-012670950-6/50004-7).
- 643 85. J. G. Maisey, An evaluation of jaw suspension in sharks. *American Museum novitates* **2706**; no.
644 2706. (1980).
- 645 86. P. Motta, C. Wilga, Advances in the Study of Feeding Behaviors, Mechanisms, and
646 Mechanics of Sharks. *Environmental Biology of Fishes* **60**, 131–156 (2001).
- 647 87. C. Wilga, P. Motta, C. Sanford, Evolution and ecology of feeding in elasmobranchs.
648 *Integrative and comparative biology* **47**, 55–69 (2007).
- 649 88. J. Huang, *et al.*, A novel data filtering method resolves the controversy in the phylogeny of
650 the Chondrichthyes. [Preprint] (2025). Available at:

- 651 <https://www.biorxiv.org/content/10.1101/2025.08.19.671162v1> [Accessed 24 October
652 2025].
- 653 89. M. Schartl, *et al.*, The genomes of all lungfish inform on genome expansion and tetrapod
654 evolution. *Nature* 1–8 (2024). <https://doi.org/10.1038/s41586-024-07830-1>.
- 655 90. A. Meyer, *et al.*, Giant lungfish genome elucidates the conquest of land by vertebrates.
656 *Nature* **590**, 284–289 (2021).
- 657 91. H. Brinkmann, B. Venkatesh, S. Brenner, A. Meyer, Nuclear protein-coding genes support
658 lungfish and not the coelacanth as the closest living relatives of land vertebrates.
659 *Proceedings of the National Academy of Sciences* **101**, 4900–4905 (2004).
- 660 92. N. Takezaki, H. Nishihara, Support for Lungfish as the Closest Relative of Tetrapods by Using
661 Slowly Evolving Ray-Finned Fish as the Outgroup. *Genome Biol Evol* **9**, 93–101 (2017).
- 662 93. N. Takezaki, F. Figueroa, Z. Zaleska-Rutczynska, N. Takahata, J. Klein, The Phylogenetic
663 Relationship of Tetrapod, Coelacanth, and Lungfish Revealed by the Sequences of Forty-
664 Four Nuclear Genes. *Molecular Biology and Evolution* **21**, 1512–1524 (2004).
- 665 94. I. Irisarri, *et al.*, Phylotranscriptomic consolidation of the jawed vertebrate timetree. *Nat*
666 *Ecol Evol* **1**, 1370–1378 (2017).
- 667 95. M.-Y. Chen, D. Liang, P. Zhang, Selecting Question-Specific Genes to Reduce Incongruence
668 in Phylogenomics: A Case Study of Jawed Vertebrate Backbone Phylogeny. *Systematic*
669 *Biology* **64**, 1104–1120 (2015).
- 670 96. T. J. Near, *et al.*, Resolution of ray-finned fish phylogeny and timing of diversification. *Proc.*
671 *Natl. Acad. Sci. U.S.A.* **109**, 13698–13703 (2012).
- 672 97. R. Betancur-R, *et al.*, The Tree of Life and a New Classification of Bony Fishes. *PLoS Curr*
673 (2013). <https://doi.org/10.1371/currents.tol.53ba26640df0ccee75bb165c8c26288>.
- 674 98. Z. Musilova, *et al.*, Vision using multiple distinct rod opsins in deep-sea fishes. *Science* **364**,
675 588–592 (2019).
- 676 99. A. Dornburg, T. J. Near, The Emerging Phylogenetic Perspective on the Evolution of
677 Actinopterygian Fishes. *Annual Review of Ecology, Evolution, and Systematics* **52**, 427–452
678 (2021).
- 679 100. M. Zhu, *et al.*, The oldest articulated osteichthyan reveals mosaic gnathostome characters.
680 *Nature* **458**, 469–474 (2009).
- 681 101. J. Lu, S. Giles, M. Friedman, J. L. den Blaauwen, M. Zhu, The Oldest Actinopterygian
682 Highlights the Cryptic Early History of the Hyperdiverse Ray-Finned Fishes. *Current*
683 *Biology* **26**, 1602–1608 (2016).

- 684 102. X. Cui, M. Friedman, T. Qiao, Y. Yu, M. Zhu, The rapid evolution of lungfish durophagy. *Nat*
685 *Commun* **13**, 2390 (2022).
- 686 103. W. Zhao, X. Zhang, G. Jia, Y. Shen, M. Zhu, The Silurian-Devonian boundary in East Yunnan
687 (South China) and the minimum constraint for the lungfish-tetrapod split. *Science China.*
688 *Life sciences* **64**, 1 (2021).
- 689 104. P. C. Sternes, L. Schmitz, T. E. Higham, The rise of pelagic sharks and adaptive evolution of
690 pectoral fin morphology during the Cretaceous. *Current Biology* **34**, 2764-2772.e3 (2024).
- 691 105. B. Brée, F. L. Condamine, G. Guinot, Combining palaeontological and neontological data
692 shows a delayed diversification burst of carcharhiniform sharks likely mediated by
693 environmental change. *Sci Rep* **12**, 21906 (2022).
- 694 106. L. A. Buatois, *et al.*, “The Mesozoic Marine Revolution” in *The Trace-Fossil Record of Major*
695 *Evolutionary Events: Volume 2: Mesozoic and Cenozoic*, M. G. Mángano, L. A. Buatois, Eds.
696 (Springer Netherlands, 2016), pp. 19–134.
- 697 107. G. J. Vermeij, The Mesozoic Marine Revolution: Evidence from Snails, Predators and
698 Grazers. *Paleobiology* **3**, 245–258 (1977).
- 699 108. L. S. TACKETT, LATE TRIASSIC DUROPHAGY AND THE ORIGIN OF THE MESOZOIC MARINE
700 REVOLUTION. *PALAIOS* **31**, 122–124 (2016).
- 701 109. S. E. Walker, C. E. Brett, Post-Paleozoic Patterns in Marine Predation: Was there a Mesozoic
702 and Cenozoic Marine Predatory Revolution? *The Paleontological Society Papers* **8**, 119–
703 194 (2002).
- 704 110. J. H. Gayford, *et al.*, Habitat Availability, Jurassic and Cretaceous Origins of the Deep-
705 Bodied Shark Morphotype and the Rise of Pelagic Sharks. *Ecology and Evolution* **15**,
706 e72082 (2025).
- 707 111. M. Bazzi, *et al.*, Early gigantic lamniform marks the onset of mega-body size in modern
708 shark evolution. *Commun Biol* **8**, 1499 (2025).
- 709 112. E. C. Miller, *et al.*, Alternating regimes of shallow and deep-sea diversification explain a
710 species-richness paradox in marine fishes. *Proceedings of the National Academy of*
711 *Sciences* **119**, e2123544119 (2022).
- 712 113. S. T. Friedman, M. M. Muñoz, A latitudinal gradient of deep-sea invasions for marine fishes.
713 *Nat Commun* **14**, 773 (2023).
- 714 114. A. R. Tanner, *et al.*, Molecular clocks indicate turnover and diversification of modern
715 coleoid cephalopods during the Mesozoic Marine Revolution. *Proceedings of the Royal*
716 *Society B: Biological Sciences* **284**, 20162818 (2017).

- 717 115. P. M. Sander, *et al.*, Early giant reveals faster evolution of large body size in ichthyosaurs
718 than in cetaceans. *Science* **374**, eabf5787 (2021).
- 719 116. R. Motani, The Evolution of Marine Reptiles. *Evo Edu Outreach* **2**, 224–235 (2009).
- 720 117. R. Motani, *et al.*, A basal ichthyosauriform with a short snout from the Lower Triassic of
721 China. *Nature* **517**, 485–488 (2015).
- 722 118. R. Motani, D. Jiang, A. Tintori, C. Ji, J. Huang, Pre- versus post-mass extinction divergence
723 of Mesozoic marine reptiles dictated by time-scale dependence of evolutionary rates.
724 *Proceedings of the Royal Society B: Biological Sciences* **284**, 20170241 (2017).
- 725 119. T. L. Stubbs, *et al.*, Ecological opportunity and the rise and fall of crocodylomorph
726 evolutionary innovation. *Proceedings of the Royal Society B: Biological Sciences* **288**,
727 20210069 (2021).
- 728 120. M. M. Johnson, D. Foffa, M. T. Young, S. L. Brusatte, The ecological diversification and
729 evolution of Teleosauroidea (Crocodylomorpha, Thalattosuchia), with insights into their
730 mandibular biomechanics. *Ecology and Evolution* **12**, e9484 (2022).
- 731 121. J. A. Schwab, *et al.*, Inner ear sensory system changes as extinct crocodylomorphs
732 transitioned from land to water. *Proceedings of the National Academy of Sciences* **117**,
733 10422–10428 (2020).
- 734 122. E. W. Wilberg, A. H. Turner, C. A. Brochu, Evolutionary structure and timing of major
735 habitat shifts in Crocodylomorpha. *Sci Rep* **9**, 514 (2019).
- 736 123. A. R. D. Payne, P. D. Mannion, G. T. Lloyd, K. E. Davis, Decoupling speciation and extinction
737 reveals both abiotic and biotic drivers shaped 250 million years of diversity in crocodile-
738 line archosaurs. *Nat Ecol Evol* **8**, 121–132 (2024).
- 739 124. J. A. MacLaren, R. F. Bennion, N. Bardet, V. Fischer, Global ecomorphological restructuring
740 of dominant marine reptiles prior to the Cretaceous–Palaeogene mass extinction.
741 *Proceedings of the Royal Society B: Biological Sciences* **289**, 20220585 (2022).
- 742 125. S. R. R. Cross, B. C. Moon, T. L. Stubbs, E. J. Rayfield, M. J. Benton, Climate, competition,
743 and the rise of mosasauroid ecomorphological disparity. *Palaeontology* **65**, e12590 (2022).
- 744 126. M. Everhart, *Rapid evolution, diversification and distribution of mosasaurs (Reptilia;*
745 *Squamata) prior to the K-T Boundary* (2005).
- 746 127. E. D. Grogan, R. Lund, *Debeerius ellefseni* (Fam. Nov., Gen. Nov., Spec. Nov.), an
747 autodiastylic chondrichthyan from the Mississippian bear gulch limestone of Montana
748 (USA), the relationships of the chondrichthyes, and comments on gnathostome evolution.
749 *J Morphol* **243**, 219–245 (2000).

- 750 128. R. Lund, E. Grogan, Relationships of the Chimaeriformes and the basal radiation of the
751 Chondrichthyes. *Rev Fish Biol Fisher* **7**, 65–123 (1997).
- 752 129. L. Frey, M. I. Coates, K. Tietjen, M. Rücklin, C. Klug, A symmoriiform from the Late Devonian
753 of Morocco demonstrates a derived jaw function in ancient chondrichthyans. *Commun*
754 *Biol* **3**, 681 (2020).
- 755 130. S. Turner, G. C. Young, Shark teeth from the Early-Middle Devonian Cravens Peak Beds,
756 Georgina Basin, Queensland. *Alcheringa: An Australasian Journal of Palaeontology* **11**,
757 233–244 (1987).
- 758 131. S. Adnet, G. Guinot, H. Cappetta, J.-L. Welcomme, Oldest evidence of bramble sharks
759 (Elasmobranchii, Echinorhinidae) in the Lower Cretaceous of southeast France and the
760 evolutionary history of orbitostylic sharks. *Cretaceous Research* **35**, 81–87 (2012).
- 761 132. S. KLUG, J. KRIWET, R. BÖTTCHER, G. SCHWEIGERT, G. DIETL, Skeletal anatomy of the
762 extinct shark *Paraorthacodus jurensis* (Chondrichthyes; Palaeospinacidae), with
763 comments on synechodontiform and palaeospinacid monophyly. *Zoological Journal of the*
764 *Linnean Society* **157**, 107–134 (2009).
- 765 133. S. Klug, Monophyly, phylogeny and systematic position of the †Synechodontiformes
766 (Chondrichthyes, Neoselachii). *Zoologica Scripta* **39**, 37–49 (2010).
- 767 134. J. Kriwet, S. Klug, A new Jurassic cow shark (Chondrichthyes, Hexanchiformes) with
768 comments on Jurassic hexanchiform systematics. *Swiss J Geosci* **104**, 107–114 (2011).
- 769 135. R. Vullo, *et al.*, Manta-like planktivorous sharks in Late Cretaceous oceans. *Science* **371**,
770 1253–1256 (2021).
- 771 136. M. Friedman, *et al.*, 100-million-year dynasty of giant planktivorous bony fishes in the
772 Mesozoic seas. *Science* **327**, 990–993 (2010).
- 773 137. D. M. Martill, *Leedsichthys problematicus*, a giant filter-feeding teleost from the Jurassic of
774 England and France. *Neues Jahrbuch für Geologie und Paläontologie - Monatshefte* 670–
775 680 (1988). <https://doi.org/10.1127/njgpm/1988/1988/670>.
- 776 138. M. Friedman, Parallel evolutionary trajectories underlie the origin of giant suspension-
777 feeding whales and bony fishes. *Proceedings of the Royal Society B: Biological Sciences*
778 **279**, 944 (2011).
- 779 139. S. J. Coatham, J. Vinther, E. J. Rayfield, C. Klug, Was the Devonian placoderm *Titanichthys* a
780 suspension feeder? *Royal Society Open Science* **7**, 200272 (2020).
- 781 140. J. Vinther, M. Stein, N. R. Longrich, D. A. T. Harper, A suspension-feeding anomalocarid
782 from the Early Cambrian. *Nature* **507**, 496–499 (2014).

- 783 141. P. Van Roy, A. C. Daley, D. E. G. Briggs, Anomalocaridid trunk limb homology revealed by a
784 giant filter-feeder with paired flaps. *Nature* **522**, 77–80 (2015).
- 785 142. A. Tajika, A. Nützel, C. Klug, The old and the new plankton: ecological replacement of
786 associations of mollusc plankton and giant filter feeders after the Cretaceous? *PeerJ* **6**,
787 e4219 (2018).
- 788 143. L. Alegret, E. Thomas, K. C. Lohmann, End-Cretaceous marine mass extinction not caused
789 by productivity collapse. *Proceedings of the National Academy of Sciences of the United*
790 *States of America* **109**, 728 (2011).
- 791 144. A. P. Martin, G. J. Naylor, Independent origins of filter-feeding in megamouth and basking
792 sharks (order Lamniformes) inferred from phylogenetic analysis of cytochrome b gene
793 sequences. *Biology of the megamouth shark* 39–50 (1997).
- 794 145. J. H. Gayford, D. J. Irschick, A. Chin, J. L. Rummer, Heterochrony and Oophagy Underlie the
795 Evolution of Giant Filter-Feeding Lamniform Sharks. *Evol Dev* **27**, e12496 (2025).
- 796 146. “A Review of Shark Reproductive Ecology: Life History and Evolutionary Implications” in
797 *Fish Reproduction*, (CRC Press, 2008), pp. 449–484.
- 798 147. “Reproductive Biology of Elasmobranchs” in *Biology of Sharks and Their Relatives*, (CRC
799 Press, 2012), pp. 307–328.
- 800 148. D. G. Blackburn, Evolution of vertebrate viviparity and specializations for fetal nutrition: A
801 quantitative and qualitative analysis. *J Morphol* **276**, 961–990 (2015).
- 802 149. L. J. V. Compagno, Alternative life-history styles of cartilaginous fishes in time and space.
803 *Environ Biol Fish* **28**, 33–75 (1990).
- 804 150. D. G. Blackburn, D. F. Hughes, Phylogenetic analysis of viviparity, matrotrophy, and other
805 reproductive patterns in chondrichthyan fishes. *Biological Reviews* **99**, 1314–1356 (2024).
- 806 151. C. G. Mull, M. W. Pennell, K. E. Yopak, N. K. Dulvy, Maternal investment evolves with larger
807 body size and higher diversification rate in sharks and rays. *Current Biology* **34**, 2773-
808 2781.e3 (2024).
- 809 152. D. Hughes, D. Blackburn, The ancestor of sharks and rays laid eggs, but ancestral state
810 reconstructions need empirically supported traits and transparent reporting: a comment
811 on Katona et al. (2023). *Journal of evolutionary biology* **38** (2025).
- 812 153. J. A. Long, K. Trinajstić, Z. Johanson, Devonian arthrodire embryos and the origin of internal
813 fertilization in vertebrates. *Nature* **457**, 1124–1127 (2009).
- 814 154. J. A. Long, K. Trinajstić, G. C. Young, T. Senden, Live birth in the Devonian period. *Nature*
815 **453**, 650–652 (2008).

- 816 155. E. D. GROGAN, R. LUND, Superfoetative viviparity in a Carboniferous chondrichthyan and
817 reproduction in early gnathostomes. *Zoological Journal of the Linnean Society* **161**, 587–
818 594 (2011).
- 819 156. J. H. Gayford, D. J. Irschick, A. Chin, J. L. Rummer, Heterochrony and Oophagy Underlie the
820 Evolution of Giant Filter-Feeding Lamniform Sharks. *Evolution & Development* **27**, e12496
821 (2025).
- 822 157. S. Nowoshilow, *et al.*, The axolotl genome and the evolution of key tissue formation
823 regulators. *Nature* **554**, 50–55 (2018).
- 824 158. B. Zuo, L. M. Nneji, Y.-B. Sun, Comparative genomics reveals insights into anuran genome
825 size evolution. *BMC Genomics* **24**, 379 (2023).
- 826 159. W. Chen, *et al.*, Chromosome-level genome assembly of a high-altitude-adapted frog (*Rana*
827 *kukunoris*) from the Tibetan plateau provides insight into amphibian genome evolution
828 and adaptation. *Frontiers in Zoology* **20**, 1 (2023).
- 829 160. H. C. Liedtke, D. J. Gower, M. Wilkinson, I. Gomez-Mestre, Macroevolutionary shift in the
830 size of amphibian genomes and the role of life history and climate. *Nat Ecol Evol* **2**, 1792–
831 1799 (2018).
- 832 161. K. O. Chan, C. R. Hutter, P. L. Wood, L. L. Grismer, R. M. Brown, Larger, unfiltered datasets
833 are more effective at resolving phylogenetic conflict: Introns, exons, and UCEs resolve
834 ambiguities in Golden-backed frogs (*Anura*: Ranidae; genus *Hylarana*). *Molecular*
835 *Phylogenetics and Evolution* **151**, 106899 (2020).
- 836 162. K. de Queiroz, P. Cantino, *International Code of Phylogenetic Nomenclature (PhyloCode)*
837 (CRC Press, 2020).
- 838 163. C. D. Brownstein, T. J. Near, Toward a Phylogenetic Taxonomy of Sturgeons
839 (*Acipenseriformes*: *Acipenseridae*). *pbmb* **66**, 3–23 (2025).
- 840 164. T. J. Near, C. E. Thacker, Phylogenetic classification of living and fossil ray-finned fishes
841 (*Actinopterygii*). *Bulletin of the Peabody Museum of Natural History* **65**, 3–302 (2024).
- 842 165. T. J. Near, C. D. Brownstein, C. E. Thacker, P. C. Wainwright, Phylogenetic Taxonomy of
843 Wrasses and Parrotfishes (*Labridae*). *pbmb* **66**, 263–338 (2025).
- 844 166. C. D. Brownstein, T. J. Near, R. P. Dearden, The Palaeozoic assembly of the holocephalan
845 body plan far preceded post-Cretaceous radiations into the ocean depths. *Proceedings of*
846 *the Royal Society B: Biological Sciences* **291**, 20241824 (2024).
- 847 167. M. Thines, *et al.*, Setting scientific names at all taxonomic ranks in italics facilitates their
848 quick recognition in scientific papers. *IMA Fungus* **11**, 25 (2020).

- 849 168. B. C. Faircloth, PHYLUCE is a software package for the analysis of conserved genomic loci.
850 *Bioinformatics* **32**, 786–788 (2016).
- 851 169. C. Tumescheit, A. E. Firth, K. Brown, ClAlign: A highly customisable command line tool to
852 clean, interpret and visualise multiple sequence alignments. *PeerJ* **10**, e12983 (2022).
- 853 170. J. L. Steenwyk, Y. Li, X. Zhou, X.-X. Shen, A. Rokas, Incongruence in the phylogenomics era.
854 *Nat Rev Genet* **24**, 834–850 (2023).
- 855 171. M. Manni, M. R. Berkeley, M. Seppey, F. A. Simão, E. M. Zdobnov, BUSCO Update: Novel
856 and Streamlined Workflows along with Broader and Deeper Phylogenetic Coverage for
857 Scoring of Eukaryotic, Prokaryotic, and Viral Genomes. *Mol Biol Evol* **38**, 4647–4654
858 (2021).
- 859 172. M. Manni, M. R. Berkeley, M. Seppey, E. M. Zdobnov, BUSCO: Assessing Genomic Data
860 Quality and Beyond. *Current Protocols* **1**, e323 (2021).
- 861 173. K. Katoh, D. M. Standley, MAFFT multiple sequence alignment software version 7:
862 improvements in performance and usability. *Mol Biol Evol* **30**, 772–780 (2013).
- 863 174. F. Ronquist, *et al.*, MrBayes 3.2: Efficient Bayesian Phylogenetic Inference and Model
864 Choice Across a Large Model Space. *Systematic Biology* **61**, 539–542 (2012).
- 865 175. A. Rambaut, A. J. Drummond, D. Xie, G. Baele, M. A. Suchard, Posterior Summarization in
866 Bayesian Phylogenetics Using Tracer 1.7. *Systematic Biology* **67**, 901–904 (2018).
- 867 176. B. Q. Minh, *et al.*, IQ-TREE 2: New Models and Efficient Methods for Phylogenetic Inference
868 in the Genomic Era. *Molecular Biology and Evolution* **37**, 1530–1534 (2020).
- 869 177. L.-T. Nguyen, H. A. Schmidt, A. von Haeseler, B. Q. Minh, IQ-TREE: A Fast and Effective
870 Stochastic Algorithm for Estimating Maximum-Likelihood Phylogenies. *Mol Biol Evol* **32**,
871 268–274 (2015).
- 872 178. R. Lanfear, P. B. Frandsen, A. M. Wright, T. Senfeld, B. Calcott, PartitionFinder 2: New
873 Methods for Selecting Partitioned Models of Evolution for Molecular and Morphological
874 Phylogenetic Analyses. *Molecular Biology and Evolution* **34**, 772–773 (2017).
- 875 179. S. Kalyaanamoorthy, B. Q. Minh, T. K. F. Wong, A. von Haeseler, L. S. Jermiin, ModelFinder:
876 fast model selection for accurate phylogenetic estimates. *Nat Methods* **14**, 587–589
877 (2017).
- 878 180. C. Zhang, M. Rabiee, E. Sayyari, S. Mirarab, ASTRAL-III: polynomial time species tree
879 reconstruction from partially resolved gene trees. *BMC Bioinformatics* **19**, 153 (2018).
- 880 181. B. Q. Minh, M. W. Hahn, R. Lanfear, New Methods to Calculate Concordance Factors for
881 Phylogenomic Datasets. *Molecular Biology and Evolution* **37**, 2727–2733 (2020).

- 882 182. R. Bouckaert, *et al.*, BEAST 2.5: An advanced software platform for Bayesian evolutionary
883 analysis. *PLOS Computational Biology* **15**, e1006650 (2019).
- 884 183. R. Bouckaert, *et al.*, BEAST 2: A Software Platform for Bayesian Evolutionary Analysis. *PLoS*
885 *Comput Biol* **10**, e1003537 (2014).
- 886 184. A. Gavryushkina, *et al.*, Bayesian Total-Evidence Dating Reveals the Recent Crown Radiation
887 of Penguins. *Syst Biol* **66**: 57-73 (2016). <https://doi.org/10.1093/sysbio/syw060>.
- 888 185. P. S. Andreev, *et al.*, Spiny chondrichthyan from the lower Silurian of South China. *Nature*
889 **609**, 969–974 (2022).
- 890 186. S. C. Morris, J.-B. Caron, A primitive fish from the Cambrian of North America. *Nature* **512**,
891 419–422 (2014).
- 892 187. S. Magallón, M. J. Sanderson, Absolute diversification rates in angiosperm clades. *Evolution*
893 **55**, 1762–1780 (2001).
- 894 188. Eschmeyer’s Catalog of Fishes | California Academy of Sciences. (2024). Available at:
895 <https://www.calacademy.org/scientists/projects/eschmeyers-catalog-of-fishes> [Accessed
896 14 February 2024].
- 897 189. L. J. Revell, phytools: an R package for phylogenetic comparative biology (and other things).
898 *Methods in Ecology and Evolution* **3**, 217–223 (2012).
- 899 190. L. J. Revell, phytools 2.0: an updated R ecosystem for phylogenetic comparative methods
900 (and other things). *PeerJ* **12**, e16505 (2024).
- 901 191. L. J. Harmon, J. T. Weir, C. D. Brock, R. E. Glor, W. Challenger, GEIGER: investigating
902 evolutionary radiations. *Bioinformatics* **24**, 129–131 (2008).

903 **Figure 1. Phylogenomic analysis reveals chondrichthyan relationships.** (A) Comparison of
904 tree topologies generated using ASTRAL-III using BUSCOs and UCEs. (B) Comparison
905 of nodal support for selected nodes across different phylogenetic methodologies and
906 different sequence dataset completeness levels. (C) Comparisons of nucleotide base pair
907 content across datasets.

908 **Figure 2. Time calibrated phylogeny of cartilaginous vertebrates.** Shown is the time-
909 calibrated phylogeny of *Chondrichthyes* made by using a Bayesian node-dating approach in
910 BEAST 2.6.6 to calibrate the ASTRAL-III multispecies coalescent phylogeny of cartilaginous
911 fishes based on 356 ultraconserved elements. Bars at nodes denote 95% highest posterior density
912 intervals for divergence times. Dotted branch indicates region of ASTRAL-III phylogeny that
913 differs from the topology generated using different partitioning approaches in IQ-TREE2.
914 Illustrations are public domain.

915 **Figure 3. Evolution of chondrichthyan ecology and life history.** Phylogenetic ancestral state
916 reconstructions of (A) ecological category and (B) parity mode along the time-calibrated

917 phylogeny of *Chondrichthyes* generated using 356 ultraconserved elements. Illustrations are
918 public domain.

919

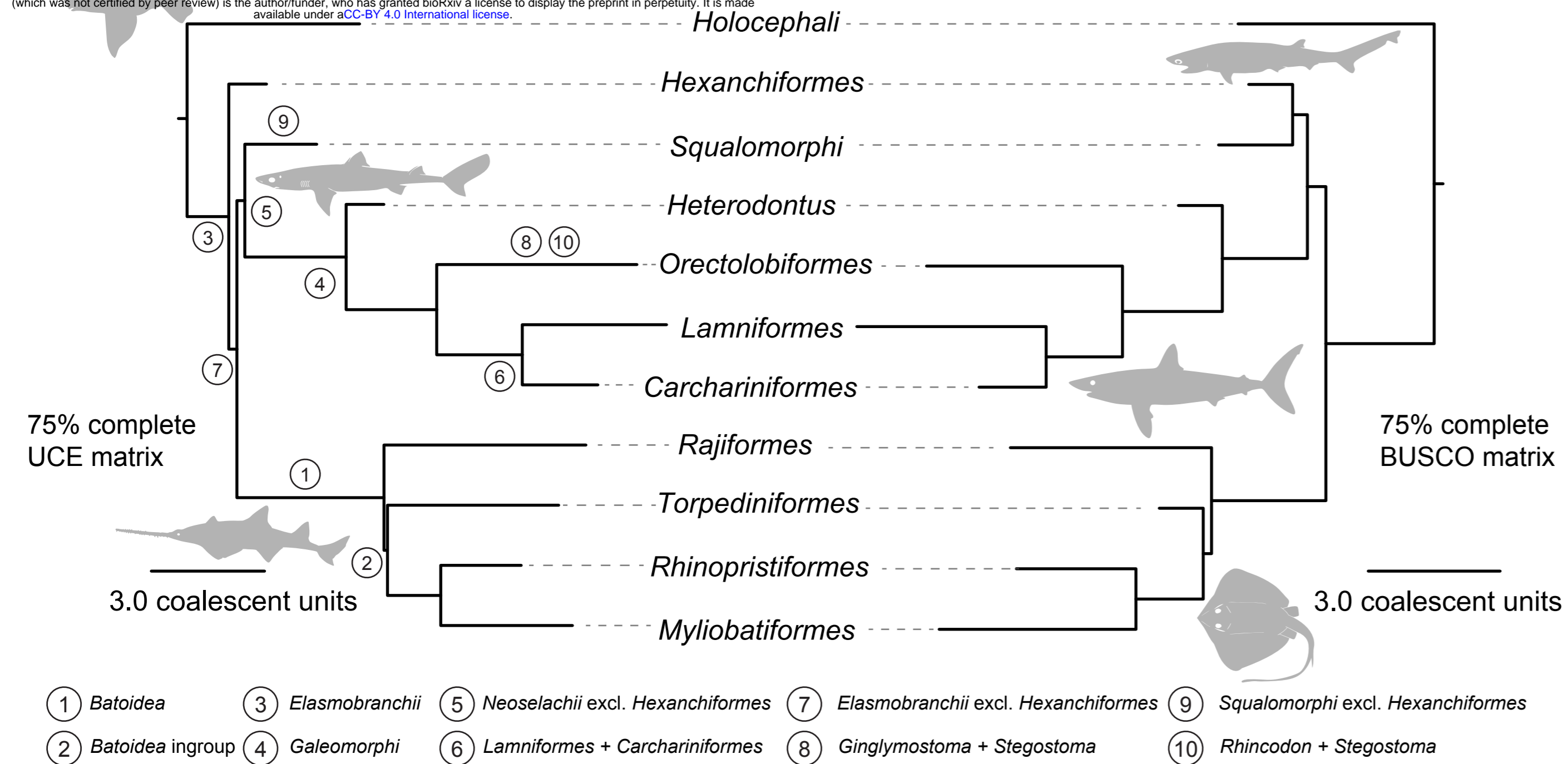
920 **Figure 4. Evolution of chondrichthyan genome size.** Traitgram of natural-log-transformed
921 genome weight in picograms made along the time-calibrated phylogeny of *Chondrichthyes*
922 generated using 356 ultraconserved elements. Illustrations are public domain.

923

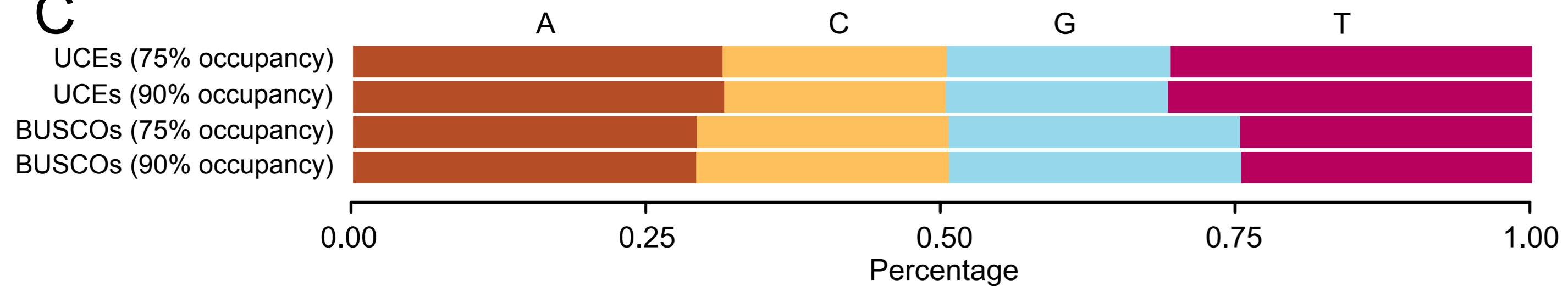
924 **Table 1.**

A

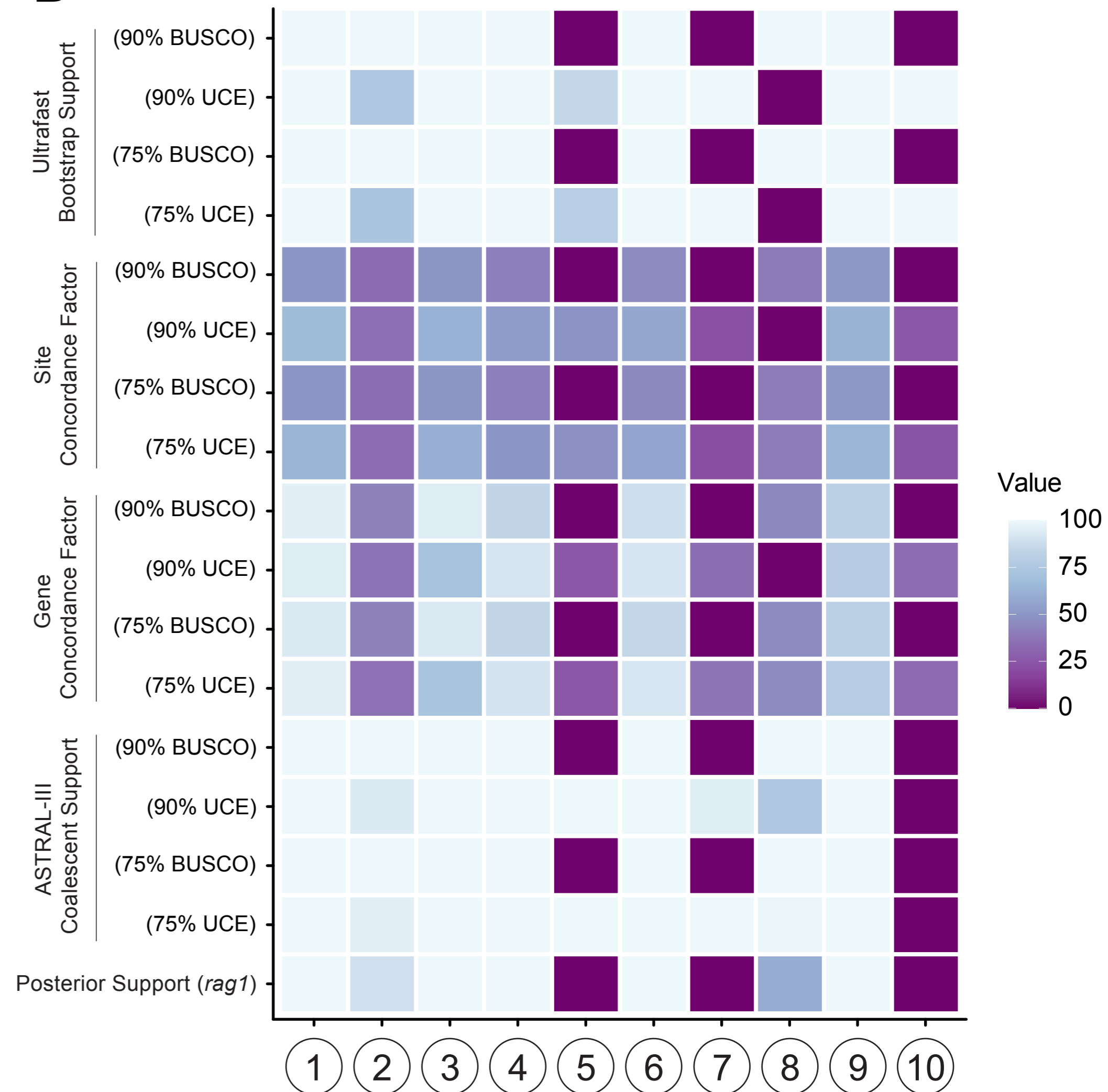
bioRxiv preprint doi: <https://doi.org/10.64898/2026.02.13.705779>; this version posted February 15, 2026. The copyright holder for this preprint (which was not certified by peer review) is the author/funder, who has granted bioRxiv a license to display the preprint in perpetuity. It is made available under aCC-BY 4.0 International license.

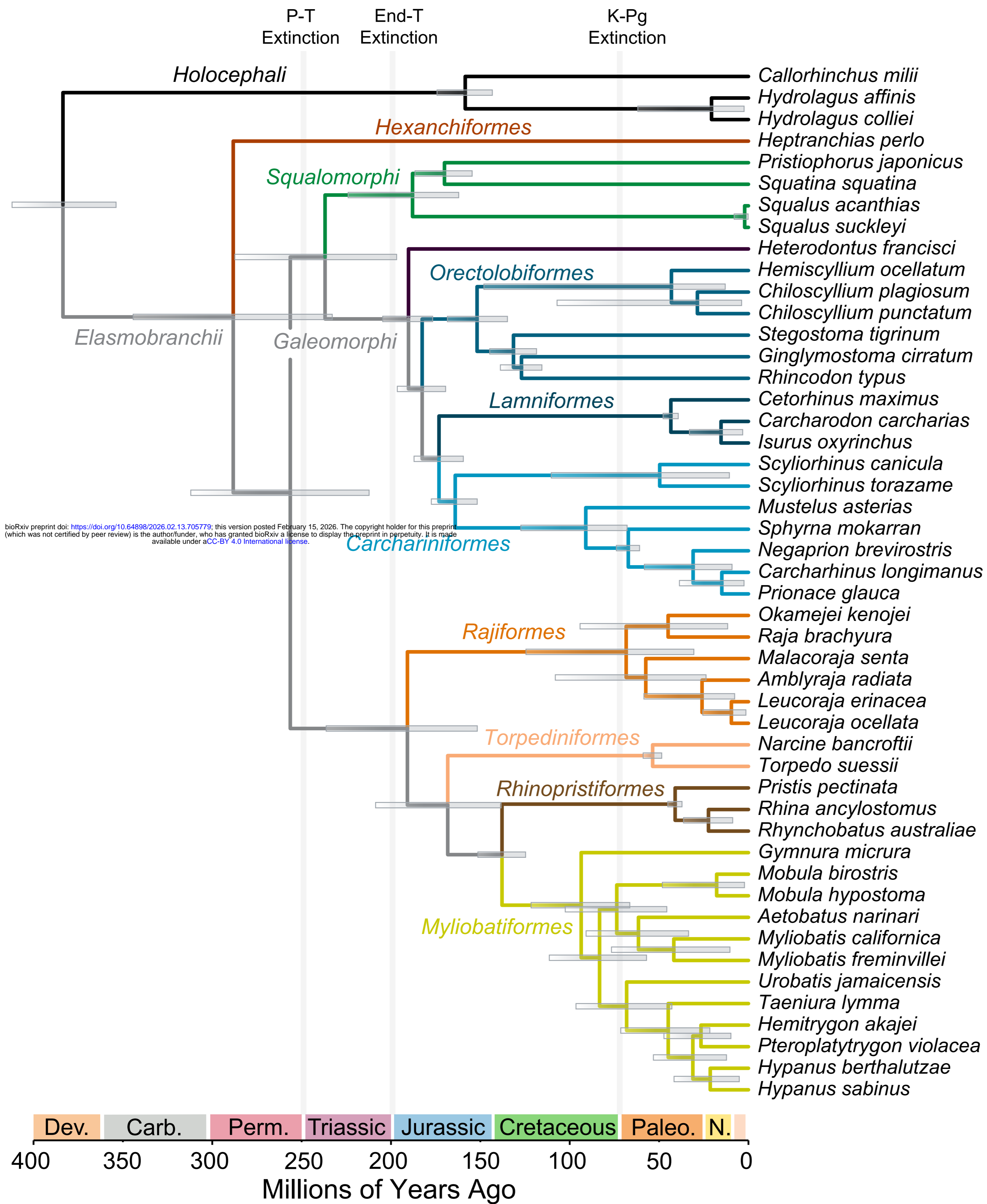


C

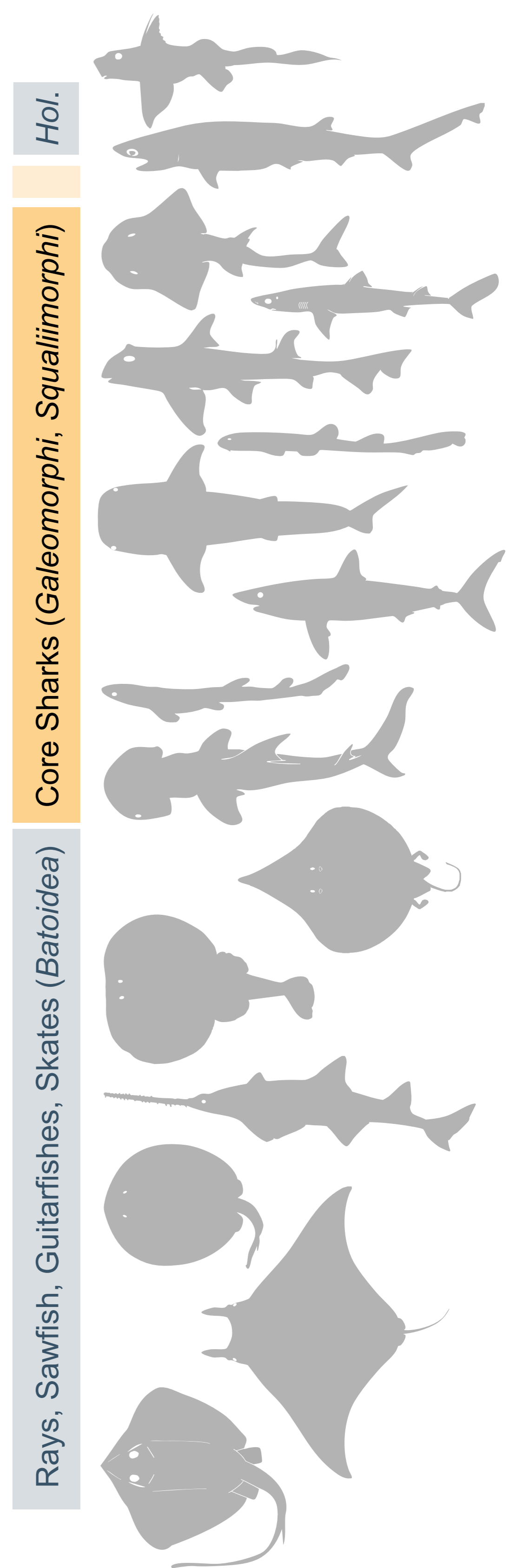


B





bioRxiv preprint doi: <https://doi.org/10.64898/2026.02.13.705779>; this version posted February 15, 2026. The copyright holder for this preprint (which was not certified by peer review) is the author/funder, who has granted bioRxiv a license to display the preprint in perpetuity. It is made available under aCC-BY 4.0 International license.

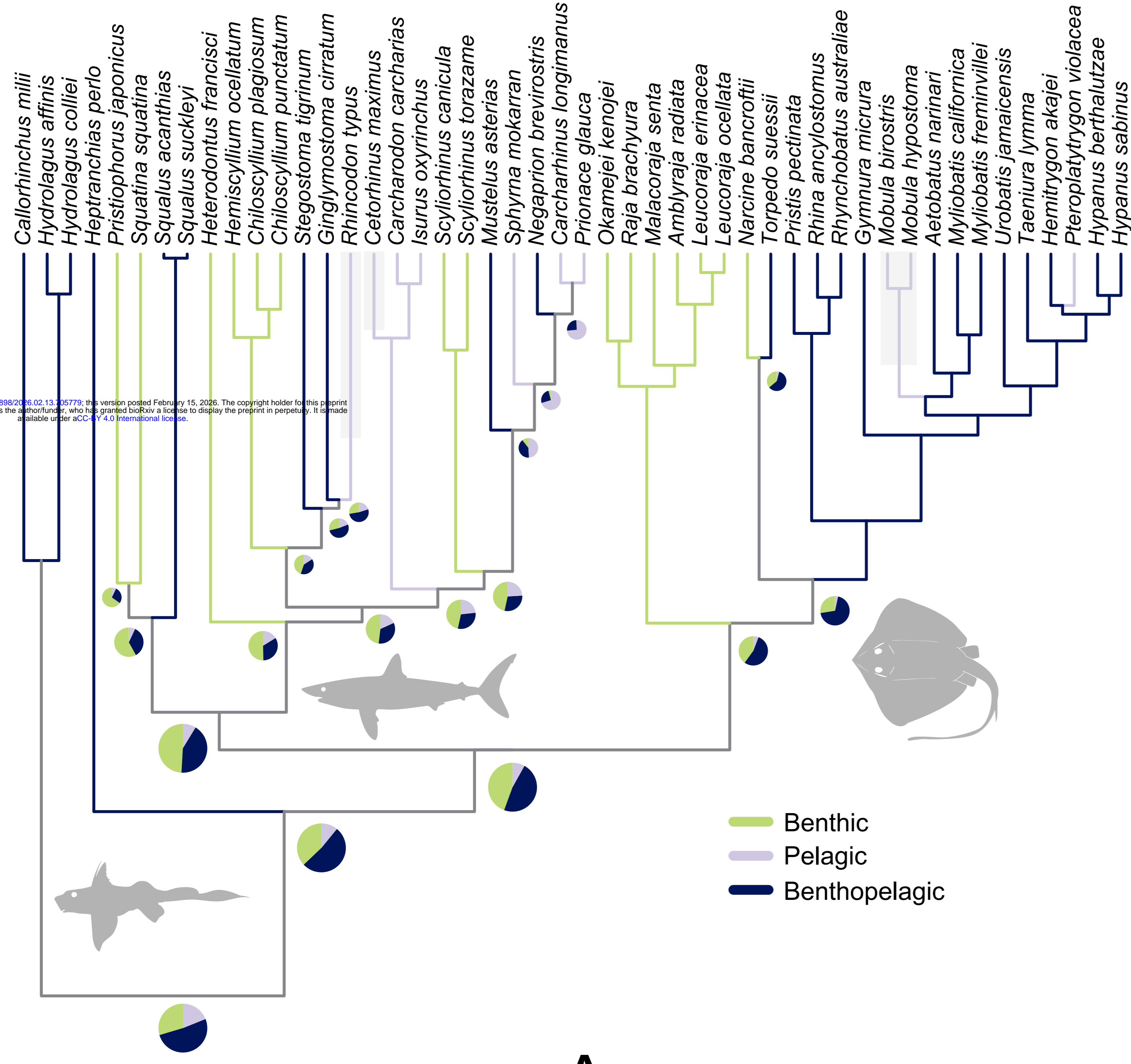


Hol.
Core Sharks (Galeomorphi, Squalimorphi)
Rays, Sawfish, Guitarfishes, Skates (Batoidea)

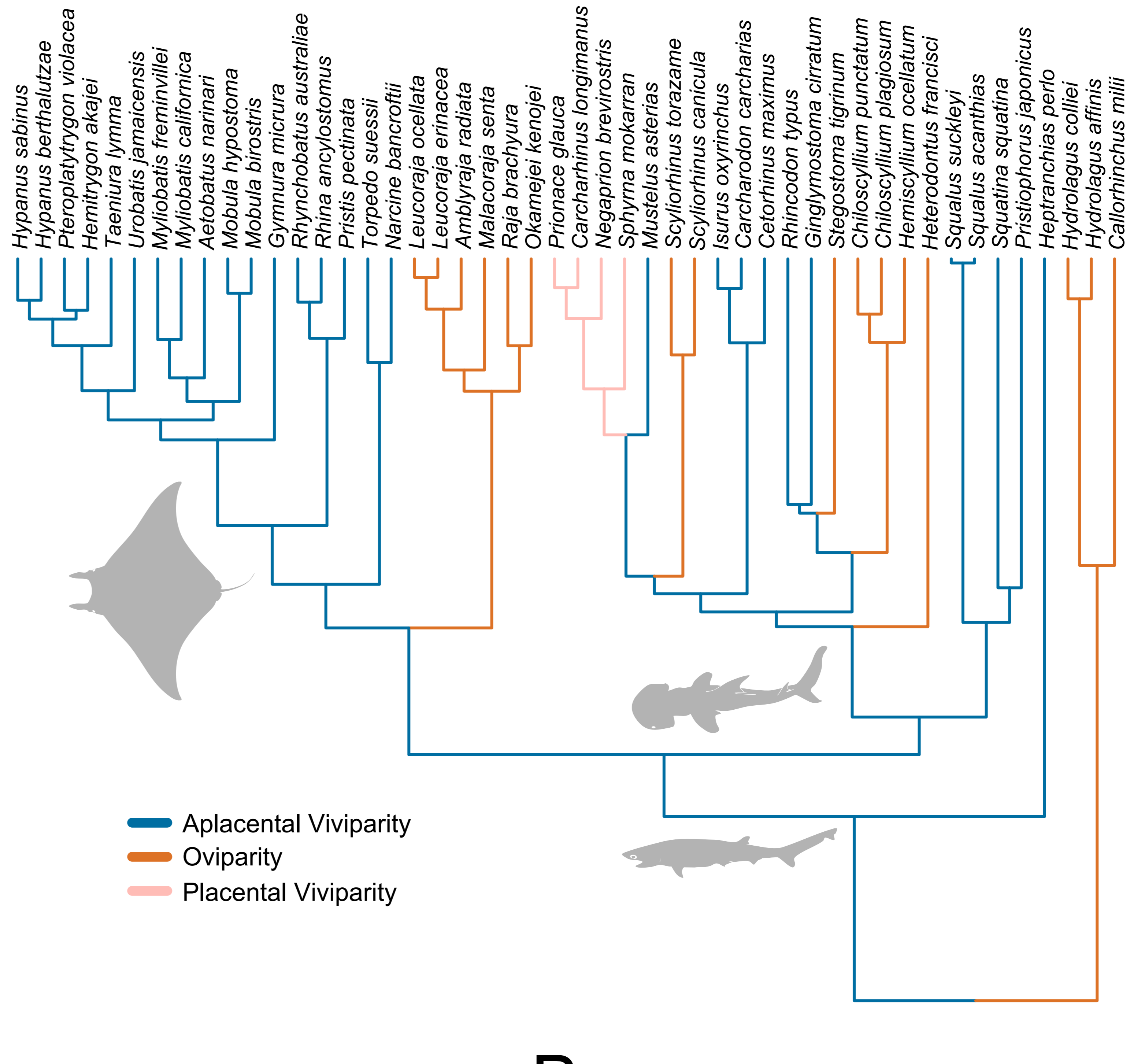
Millions of Years Ago

400 350 300 250 200 150 100 50 0

Dev. Carb. Perm. Triassic Jurassic Cretaceous Paleo. N.



A



Millions of Years Ago

400 350 300 250 200 150 100 50 0

Dev. Carb. Perm. Triassic Jurassic Cretaceous Paleo. N.

B

